Dragging of Liquid Bi Paticles induced by Grain Boundary Migration in Al-Bi Alloys

Dragging of Liquid Bi Particles Induced by Grain Boundary Migration in Al–Bi Alloys[*1]

Ryosuke Kainuma[1,*2], Ikuo Ohnuma[1] and Kiyohito Ishida[2]

[1]*Department of Materials Science, Graduate School of Engineering, Tohoku University, Sendai 980-8579, Japan*
[2]*NICHe, Tohoku University, Sendai 980-8579, Japan*

Microstructure and grain growth characteristics of pre-deformed Al–Bi alloys annealed at 773 K were investigated mainly by scanning electron microscopic (SEM) observation. In addition to very fine liquid-Bi particles in the grains, large Bi particles were observed on the grain boundaries, and non-precipitation zones are mainly formed in the vicinity outside of the curved grain boundaries. This result suggests that the Bi particles on the grain boundaries were dragged by the grain boundaries. The grain growth is significantly retarded by the effect of this dragging, the origin of which can be explained by the decrease of the interfacial energy of the intragranular Bi particles. Quantitative analysis showed that the diffusion of Al atoms in the liquid Bi particles on the grain boundaries is the rate-determining process of this dragging.

1. Introduction

Recently, it has been reported by Koike *et al.* that Al alloys which include a small amount of Bi show a superplasticity of about 200% in the temperature region above 543 K.[1,2] Since the compositions of these alloys are located in the two-phase region of Al (fcc) + liquid Bi as shown in Fig. 1,[3] liquid Bi particles are expected to be dispersed in the Al matrix at temperatures above 543 K. They have suggested that the liquid Bi phase existing on the grain boundaries may play an important role in obtaining the superplasticity.[1] However, there have been no reports on grain growth and microstructural evolution during annealing of Al–Bi binary alloys.

The particles on the grain boundaries constrain grain growth due to the so-called pinning effect, regardless of whether the particles are solid or liquid. This effect means that the grain boundary particles always receive some force from the grain boundaries which acts on the particles and cause them to migrate with the grain boundaries. With regard to Cu alloys containing some number of liquid oxide particles, Ashby and Centamore[4] reported that the liquid particles on the grain boundaries are dragged by grain boundary migration, and that the average dragging distance is strongly dependent on the viscosity of the particles. The same kind of phenomenon was reported in Fe–Ni–Cr–C[5] and Cu–Al–O.[6] Subsequently, Geguzin and Krivoglaz[7] and Gottstein and Shvindlerman[8] theoretically analyzed this phenomenon and proposed some formulae to describe the mobility of a spherical particle receiving an external force.

In the present paper, recrystallization and grain growth characteristics in Al–Bi alloys were studied, and it was found that dragging of liquid particles due to grain boundary migration also occurs in Al–Bi alloys.

2. Experimental Procedures

Two Al–Bi alloys with 3.5 and 6.9 mass% Bi, which were designated to be composed of 1 and 2 vol% Bi, respectively, were prepared in an induction furnace under an argon atmosphere from pure metals, *i.e.*, 99.7%Al and 99.9%Bi. All the cast alloys which have a columnar shape with a diameter of 10 mmϕ were cold-rolled up to a thickness of about 4 mm, and annealed at 773 K for recrystallization and further grain growth, the end time of the recrystallization in the annealing being estimated by the Micro-Vickers Hardness (MVH) test and metallographic examination. Microstructural observation of liquid particles was carried out mainly by scanning electron microscopy (SEM) after polishing with diamond paste. The grain boundaries were observed by optical microscopy (OM), where the electrolytic etching was performed with an etchant consisting of ethanol 70 vol% + ethyleneglycol 20 vol% + perchloric acid 10 vol% at 0°C under a current condition of DC 40 V with a stainless cathode. The mean grain size of the matrix phase was determined by optical microscope using quantitative microstructure analysis.[9]
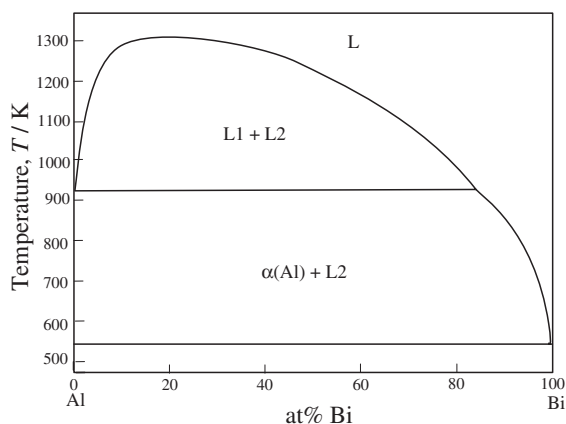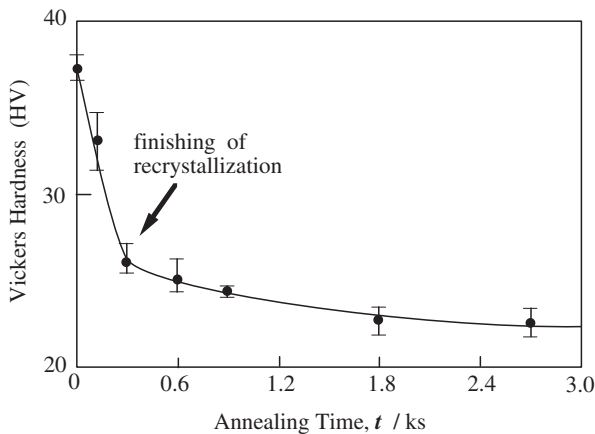

Fig. 1 Al–Bi binary phase diagram.

Fig. 2 Vickers hardness of pre-deformed Al–1 vol%Bi alloy annealed at 773 K. The hardness drastically decreases with increasing annealing time due to recrystallization in the initial stage, and the significant decrease stops at $t = 300$ s. This behavior suggests that the recrystallization is complete at about 300 s.

3. Results and Discussion

3.1 Recrystalization

Since the annealing after cold-rolling was performed at 773 K and the recrystallization process continuously changed to the grain growth mode, the time when recrystallization is complete has to be estimated. The MVH test and microstructure observation were carried out to determine the time of completion. Figure 2 shows the result of the MVH examination for the 1 vol%Bi alloy annealed at 773 K after cold-rolling. The MVH, which shows HV = 37 in the as-rolled specimen, decreases due to annealing of 300 s up to HV = 25 and levels off at about HV = 23 after annealing for 1.8 ks. Since the hardness of as-deformed specimens drastically decreases due to recrystallization in general, this result suggests that the recrystallization has already been completed by 300 s. Figures 3(a) and (b) show the SEM micrographs taken of the as-rolled specimen and of the one annealed for 300 s, respectively, where the bright contrast corresponds to Bi particles. While the microstructure of the as-deformed specimen shows the microscopic anisotropy with Bi particles prolonged in the direction parallel to the rolling, the microstructure after annealing for 300 s is almost isotropic. All these results suggest that the recrystallization is complete at 300 s. It was also confirmed in the 2 vol%Bi specimen that the time required for completion of the recrystallization is almost the same as that in the 1 vol%Bi alloy.

3.2 Grain growth

Figures 4(a) and (b) show a SEM micrograph and its corresponding OM taken of the 2 vol%Bi specimen annealed for 346 ks. The OM exhibits that the microstructure is divided into two regions, one with bright and the other with mixed contrasts. It was confirmed by SEM micrograph that the bright and mixed regions correspond to the non-precipitation and Al+Bi two-phase zones, respectively. It is interesting to note that most non-precipitation zones are located in the vicinity outside of the curved grain boundaries. These results suggest that the non-precipitation zone was formed by sweeping of the intragranular Bi particles due to grain
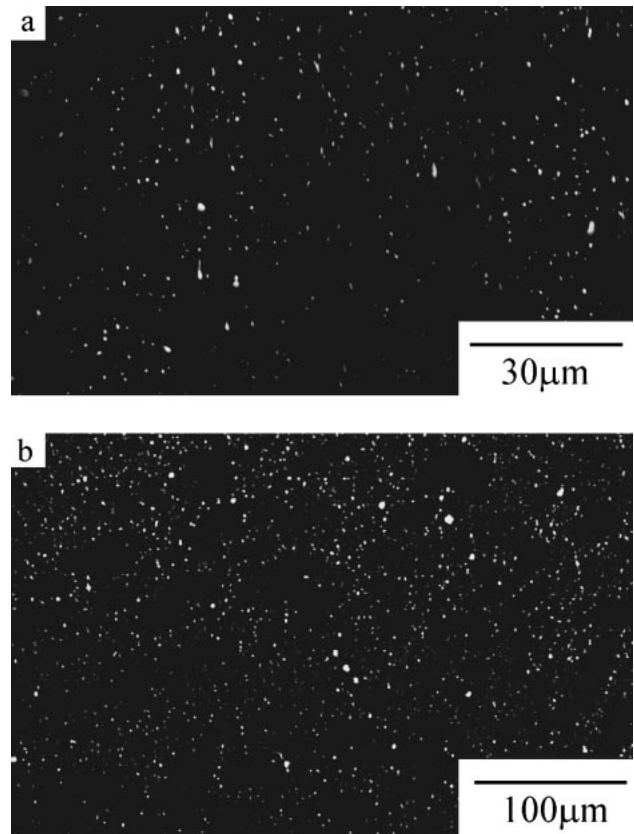

Fig. 3 SEM micrographs of Al–1 vol%Bi specimens as-rolled (a) and as-annealed at 773 K for 300 s after rolling (b). Shapes of grains and Bi particles after annealing are isotropic and the recrystallization has been completed.

boundary migration and that the Bi particles on the grain boundaries were dragged by the grain boundaries. A similar phenomenon was reported in the Cu-oxide systems by Ashby and Centamore.[4]

Figure 5 shows the variation of the mean grain radius of the 1 and 2 vol%Bi specimens with annealing time. Although the obtained data are slightly scattered, it is obviously seen that the grain radii at the same annealing time of both alloys are very small. The grain growth rate is generally expressed by

$$\overline{R}^n - \overline{R}_0^n = K \cdot t, \tag{1}$$

where t is the annealing time, $\overline{R}$ and $\overline{R}_0$ are the mean grain radii at time t and at $t = 0$, respectively, and K is a constant. By eq. (1), the slope of $\log \overline{R}$ plots against $\log t$ corresponds to $1/n$. In the grain growth of pure Al, it has been reported that the n value is around 4 (i.e., $1/n = 0.25$), as demonstrated by the data of 638 K and 679 K by Gorden and El-Bassyouni[10] in Fig. 5. In the case of the present alloys, however, the n value is about 10 ($1/n = 0.1$) and the grain growth is extremely slow. According to the Monte-Carlo simulation on grain growth of a microstructure dispersing mobile fine particles by Hassold and Srolovitz,[11] the dragged particles strongly restrain the grain growth of the matrix phase. Thus, it may be concluded that the extreme retardation of the grain growth observed in the Al–Bi alloys is due to the effect of dragging of the liquid Bi particles during grain boundary migration.
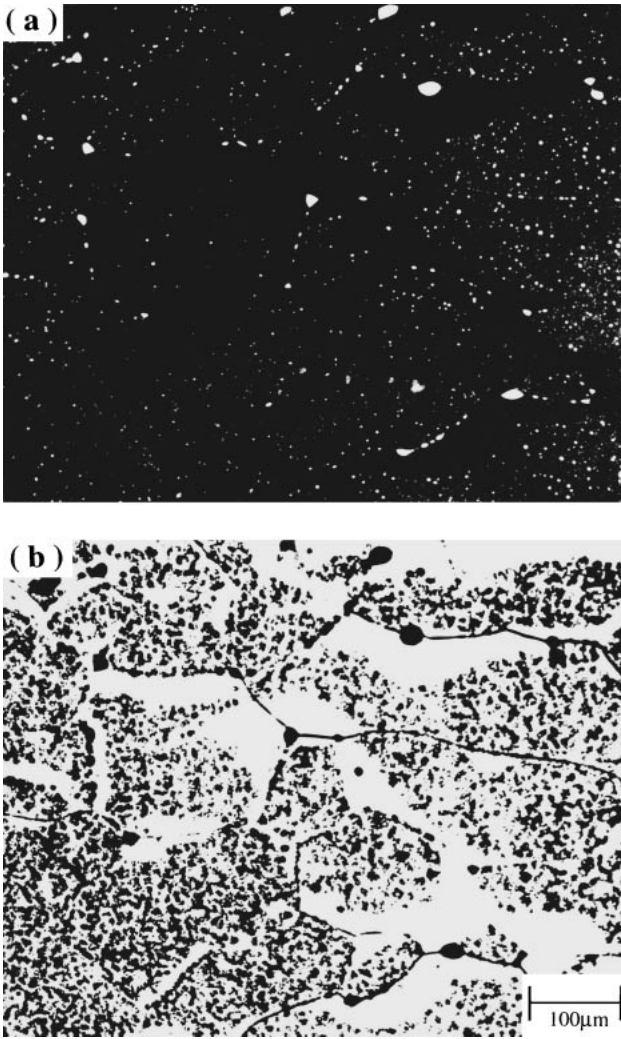
Fig. 4 SEM micrograph (a) and the corresponding optical micrograph (b) of pre-deformed Al–2 vol%Bi alloy annealed at 773 K for 3.46×10^2 ks (4 days).
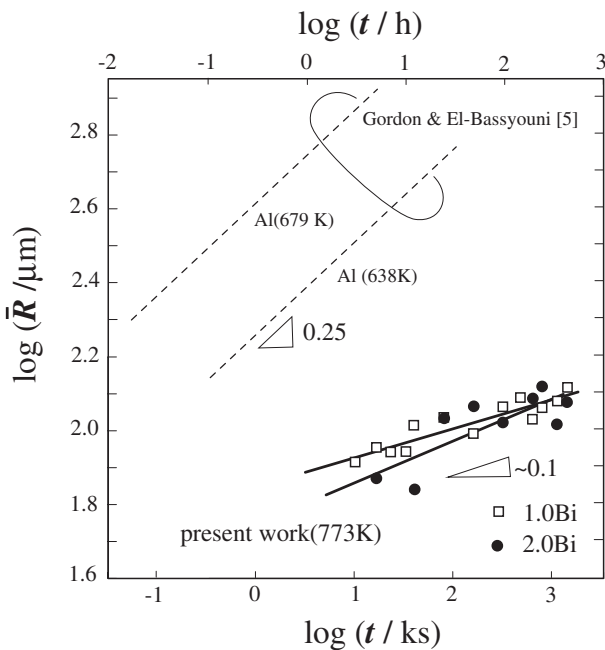
3.3 Driving force for migration of Bi particles

It is known that dispersing particles bring about the pinning effect which affects grain growth. In the case in which the mobility of the grain boundary particles is much lower than that of the grain boundaries, the driving force for grain boundary migration should be balanced with the pinning particles and each grain boundary particle may receive some force from the pinned boundary. When using the pressure P from the grain boundary acting in a normal direction of the boundary and the average number N_s of the grain boundary particles on the unit area of boundary, the driving force acting on one Bi particle on the grain boundary is given by P/N_s, and the migration rate of a dragged particle is

$$v = \frac{M \cdot P}{N_s},\qquad(2)$$

where M is the mobility of the particle.[7,8]

One of the driving forces for grain boundary migration is due to the curved grain boundaries, which is given by Gibbs-Thomson's relation:

$$P_g = \frac{2\sigma^{Al/Al}}{R_g},\qquad(3)$$

where $\sigma^{Al/Al}$ and R_g are the grain boundary energy and the radius of the grain boundary, respectively. When the most particles are located mainly on the grain boundaries, P_g would be dominant in driving force. In the present case where many very fine Bi particles exist in the grains as shown in Fig. 6, however, another effect has to be taken into account. The grain boundary migration yields a non-precipitation zone in the region through which the grain boundaries pass. Since the two-phase region along the inside of the curved grain boundary has slightly higher energy than the non-precipitation zone along the outside due to the interfacial energy between the fine Bi particles and the matrix, the grain boundary may be subject to a force which drives the
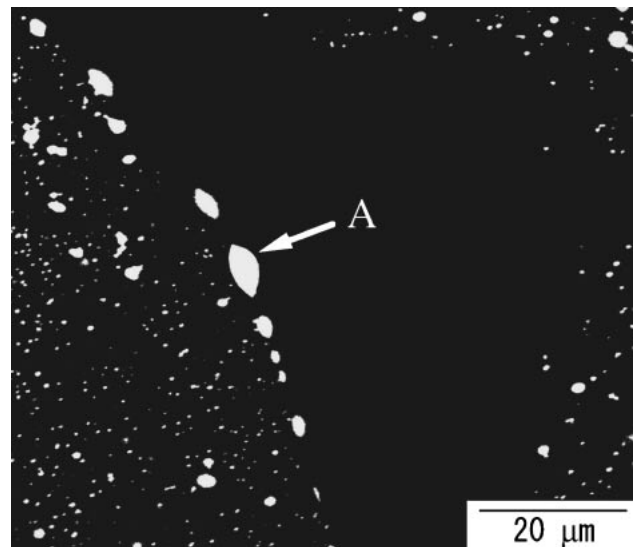

Fig. 5 Annealing time dependence of the mean grain radius.

Fig. 6 SEM micrograph of pre-deformed Al–2 vol%Bi alloy annealed at 773 K for 8.64×10^2 ks (10 days). There are very fine Bi particles in the grains.
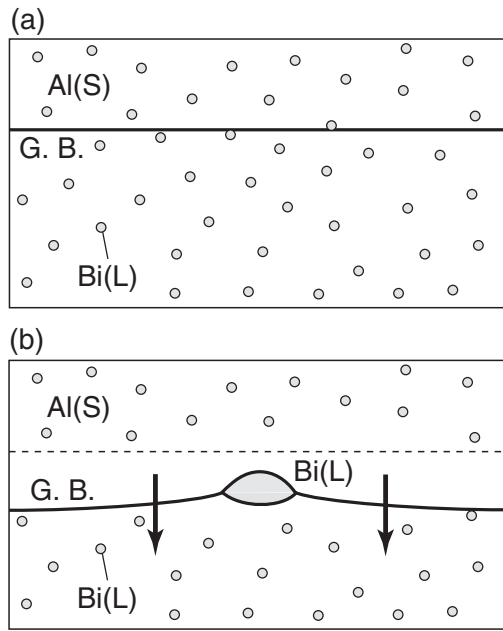
Fig. 7 Boundary migration due to the interfacial energy between the matrix and the intragranular Bi particles.

boundary in the inside direction with the two-phase structure as shown in Fig. 7(b). This situation is similar to the recrystallization whose boundaries proceed to the deformed region with a stored high energy. In this case, the contribution of this effect to grain boundary migration is given by the volume fraction f and the mean radius r_p of the intragranular Bi particles (see Appendix A),

$$P_p = \frac{3f \cdot \sigma^{Al/Bi}}{r_p}. \tag{4}$$

Consequently, the total driving force of the grain boundary migration may be obtained by the summation of the above two effects $P = P_g + P_p$.

In order to evaluate the relative contribution of P_g and P_p to the total driving force, a numerical calculation of the driving force in the specimen heat-treated under the condition of $f = 0.01$, $T = 773\,K$ and $t = 345.6\,ks$ was carried out on the basis of the experimental data obtained in this study. All the required data and the results are listed in Table 1, and the data on the interfacial energy and the molar volumes of Al and Bi are described in Appendix B. Furthermore, the R_g was estimated from the $\overline{R}$ in Fig. 5 using the relation of $R_g = 4.5\overline{R}$ reported by Haroun and Budworth;[12] the r_p was determined by SEM observation. As shown in Table 1, the P_p rather than the P_g is dominant.

3.4 Mobility of Bi particles

The mobility of a particle under a driving force in a solid matrix has been theoretically analyzed by Geguzin and Krivoglaz.[7] They reported that when a spherical particle is subject to a driving force in one direction, the compressive and tensile stress fields appear in the front and rear regions of the particle, respectively, and the particle moves in the forced direction through diffusion of atoms induced by the stress field in the matrix. According to them, three diffusional processes can be considered:

In Case I, by volume diffusion in the matrix phase surrounding the spherical particle, the mobility is given by

$$M_m = \frac{D_{vm} \cdot V_m}{RT \cdot r^3} \tag{5}$$

where D_{vm} is the volume diffusion coefficient of atoms in the matrix phase, V_m is the molar volume of the matrix phase, R and T are the gas constant and temperature, and r is the radius of the particle.

In Case II, by interfacial diffusion through the interface between the matrix and the particle,

$$M_s = \frac{D_s \cdot a \cdot V_m}{10RT \cdot r^4} \tag{6}$$

where D_s is the interfacial diffusion coefficient and a is the lattice constant of matrix.

In Case III, by the impurity diffusion of the solute atoms in the particle,

$$M_p = \frac{D_{vp} \cdot n_p \cdot V_m^2}{10RT \cdot V_p \cdot r^3} \tag{7}$$

where D_{vp} is the impurity diffusion coefficient, n_p is the mole fraction of the solute in the particle, and V_p is the molar volume of the particle phase. According to eqs. (5)–(7), the mobility of the particle is strongly affected by the particle size r, drastically decreasing with increasing size.

It is seen in Fig. 6 that while the Bi particles grasped by the grain boundaries immediately disappear, the particles already existing on the grain boundaries are very large. This result suggests that the Bi particles in contact with the boundaries are immediately dissolved and some larger particles on the grain boundaries grow by Ostwald ripening. It is interesting to note that the grain boundary is curved in the vicinity of the large particle labeled (A) in Fig. 6, which suggests that the boundary migration seems to be affected by the large particle. Although the formulae by Geguzin and Krivoglaz are given for the boundary particles with a spherical but not a lenticular shape, numerical calculation was performed using eqs. (5)–(6) to clarify the diffusion mechanism of the dragging. The estimation of data used for the calculation is described in Appendix B. The mobilities at $T = 773\,K$ obtained on a boundary Bi particle with $r = 2\,\mu m$ are $M_m =$

Table 1 Driving forces for boundary migration P_g and P_p, the migration velocity of the Bi particles v_{cal} obtained by eq. (2) and the grain boundary migration velocity v_{obs} estimated from grain growth in Fig. 5, in the Al–1 vol%Bi alloy annealed at 345.6 ks (96 h), where mean grain boundary radius is R_g, mean radius of Bi particles in the grains is r_p, mean radius of Bi particls on the grain boundaries is r and the number of Bi particles per unit area of boundary is N_s.

R_g (μm)	r_p (μm)	r (μm)	N_s (m^{-2})	P_g (J/m^3)	P_p (J/m^3)	v_{cal} (m/s)	v_{obs} (m/s)
5.0×10^2	0.25	2.0	3.0×10^{10}	1.3×10^3	8.9×10^3	2.8×10^{-10}	1.2×10^{-10}

$4.6 \times 10^{-6}\,\text{m}^2/\text{Js}$ in Case I, $M_\text{s} = 5.4 \times 10^{-6}\,\text{m}^2/\text{Js}$ in Case II and $M_\text{p} = 8.4 \times 10^{-4}\,\text{m}^2/\text{Js}$ in Case III; the M_p in Case III is about 160–180 times higher than those in the other two cases. This means, therefore, that the migration of the Bi particle may be due to the impurity diffusion of the solute Al atoms in the Bi particles.

3.5 Migration rate of Bi particles

The migration rate of the Bi particles on the grain boundaries is estimated using the relation of eq. (2). N_s is evaluated to be equal to a reciprocal value of the effective boundary area S_eff which is defined as the mean grain boundary area dominated by one Bi particle on the grain boundary,

$$N_\text{s} = 1/S_\text{eff} = c/S_\text{b}, \tag{8}$$

where $S_\text{b}(= \pi r^2)$ is the mean grain boundary area occupied by one Bi particle with the radius r on the grain boundary, and c is the area ratio of the S_b for S_eff. The c value can be easily evaluated with SEM observation, and the actual value of N_s was determined by the experimental data of c and r. The numerical values of the c, r, N_s and the calculated migration rate v_cal on the microstructure of the specimen annealed at 773 K for 345.6 ks are listed in Table 1, where the observed migration rate v_obs was evaluated by the relation of $R_\text{g} = 4.5\overline{R}$[12] on the basis of the grain growth rate shown in Fig. 5. Since the calculated value is within the same order as that of the observed one, it can be concluded that the migration model of the pinning particles, which is based on (1) the driving force due to consumption of the Bi particles in the grains and (2) the mobility dominated by the impurity diffusion of Al in the grain boundary Bi particles, is reasonable for explaining the present phenomena.

This kind of dragging phenomenon has been little reported, because the requirement on the mobility of the particle is very limited as described in eqs. (5)–(7), *i.e.*,
 (1) boundary particles should be very small,
 (2) diffusion coefficient for the particle migration should be very large,
 (3) solubility n_p of the solute atoms in the particles should be high in the case in which the impurity diffusion in the particles is dominant for the diffusion process, *etc*.

According to the paper on the dragging phenomenon in the Cu alloys with the fine oxide particles by Ashby and Centamore,[4] the liquid particles, but not the solid particles, are dragged and the mobility of the dragging particles is strongly connected with the viscosity of the liquid particle. This result can be explained in connection with the diffusivity of the solute atoms in the particles as mentioned in the above condition (2). Recently, the present authors have examined the study on the effect of dragging in the Al–In and Al–Pb systems with a phase diagram similar to that of Al–Bi, and found that the Al–In alloys show a similar effect of dragging, while the Al–Pb alloys do not. This difference may be explained by the fact that the solubility of Al in liquid Pb is relatively less than that in the liquid In. This result suggests that condition (3) is also important.

4. Conclusions

(1) The Vickers hardness of the Al-1 and 2 vol% Bi alloy specimens annealed at 773 K after cold-rolling drastically decreases until 300 s in the initial stage and then becomes steady. This result suggests that the recrystallization due to annealing at 773 K has been complete by 300 s, which was confirmed by SEM observation.
(2) The dragging of the liquid Bi particles by grain boundary migration was observed in the grain growth at 773 K.
(3) The grain growth of the Al–Bi alloys at 773 K was strongly retarded by the dragging of liquid Bi particles.
(4) The driving force for migration of the grain boundaries pinned by Bi particles is due to two factors: the grain boundary energy and the interfacial energy between the matrix and the intragranular Bi particles. In the present Al–Bi alloys, the latter is dominant.
(5) The dragging of the Bi particles due to grain boundary migration is explained as being the effect of the impurity Al diffusion in the Bi particles which is induced by the external force.

REFERENCES

1) J. Koike, K. Miki, K. Maruyama and H. Oikawa: Philos. Mag. A **78** (1998) 599–614.
2) J. Koike, K. Miki, H. Takahashi and K. Maruyama: Mater. Sci. Eng. A **285** (2000) 158–164.
3) *Binary Phase Diagrams*: 2nd ed., (eds. T. B. Massalski *et al.*), (ASM International, vol. 1 1990), p. 128.
4) M. F. Ashby and R. M. A.Centamore: Acta Metall. **16** (1968) 1081–1092.
5) E. F. Coch and K. T. Aust: Acta Metall. **15** (1967) 405–412.
6) K. K. Ziling and A. I. Grankin: Izv. Vyssh. Ucheb. Zaved., Fizika **11** (1968) 157–161.
7) Ya. E. Geguzin and M. A. Krivoglaz: *Migration of Macroscopic Inclusions in Solids*, (Consultants Bureau, New York 1973).
8) G. Gottstein and L. S. Shvindlerman: Acta Metall. Mater. **41** (1993) 3267–3275.
9) T. Sakuma and T. Nishizawa: Bulletin of the JIM **10** (1971) 279–283. (in Japanese)
10) P. Gordon and T. A. El-Bassyouni: Trans. AIME **233** (1965) 391–397.
11) G. N. Hassold and D. J. Srolovitz: Scr. Metall. Mater. **32** (1995) 1541–1547.
12) N. A. Haroun and D. W. Budworth: J. Mater. Sci. **3** (1968) 326–332.
13) L. E. Murr: *Interfacial Phenomena in Metals and Alloys*, (Addison-Wesley, Reading, 1975), p. 131.
14) N. L. Peterson: J. Nuclear Mater. **69&70** (1978) 3–37.
15) T. L. Sri Krishna, M. A. Dayananda and R. E. Grace: Metall. Trans. **2** (1971) 3355–3359.

Appendix A: Derivation of eq. (4)

Under the assumption of the random distribution of ideally spherical Bi particles with the same radius, the number of Bi particles in the unit volume is approximately described by

$$n = \frac{1}{V_{\text{eff}}} = \frac{3f}{4\pi r_{\text{p}}^3}, \tag{A·1}$$

where the V_{eff} is the effective volume dominated by one Bi particle in the grains. Since the driving force P_{p} is equal to the summation of the interfacial energy on all the particles in the unit volume:

$$P_{\text{p}} = 4\pi r_{\text{p}}^2 \cdot n \cdot \sigma^{\text{Al/Bi}}, \tag{A·2}$$

Equation (4) is given by the insertion of eq. (A·1) into eq. (A·2).

Appendix B: Parameters used for the calculation

(1) Interfacial energies $\sigma^{\text{Al/Al}}$ and $\sigma^{\text{Al/Bi}}$:

The value in the literature of random grain boundary $\sigma^{\text{Al/Al}} = 0.324\,\text{Jm}^{-2}$ [13] was used. Since there is no report on the $\sigma^{\text{Al/Bi}}$, $\sigma^{\text{Al/Bi}} = 0.2\,\text{Jm}^{-2}$ was determined by the measurement of the wet angle θ of the triple point between the Bi particle and the grain boundary in the relation $\sigma^{\text{Al/Al}} = 2\sigma^{\text{Al/Bi}} \cdot \cos\theta$, where the $\cos\theta$ was about 0.9.

(2) Molar volumes:

$V_{\text{m}} = V_{\text{Ai(s)}} = 1.05 \times 10^{-5}\,\text{m}^3 \cdot \text{mol}^{-1}$ and $V_{\text{p}} = V_{\text{Bi(s)}} = 1.66 \times 10^{-5}\,\text{m}^3 \cdot \text{mol}^{-1}$ at room temperature were used for the molar volumes of the pure Al and Bi.

(3) Diffusion coefficients D_{vm}, D_{vp}, D_{s}:

The self-diffusion and the impurity diffusion coefficients of Al, $D_{\text{vm}} = D^*_{\text{Ai in Al(s)}} = 2.3 \times 10^{-14}\,\text{m}^2 \cdot \text{s}^{-1}$ [14] and $D_{\text{vp}} = D^*_{\text{Ai in Bi(L)}} = 1.3 \times 10^{-9}\,\text{m}^2 \cdot \text{s}^{-1}$, [15] were used for the D_{vm} and the D_{vp}. Since there is no data on the interfacial diffusion D_{s}, the D_{vp} was used instead of D_{s}.

(4) The other parameters:

The solubility of Al in the liquid Bi particles: $n_{\text{Al(L)}} = 0.05$ is taken from the phase diagram and the lattice parameter in eq. (6): $a_{\text{Al}} = 4.05 \times 10^{-10}\,\text{m}$ is of fcc Al crystal at room temperature.